

Electric-Field-Induced Pockels Effect based Phase Modulator on Micron-Thick Silicon Photonic Platform

Abdulaziz E. Elfiqui^(1,*), Arijit Bera⁽²⁾, Timo Aalto⁽²⁾, Takuo Tanemura⁽¹⁾, and Yoshiaki Nakano⁽¹⁾

⁽¹⁾The University of Tokyo, 7-3-1 Hongo, Bunkyo-ku, Tokyo, Japan, *elfiqui@hotaka.t.u-tokyo.ac.jp

⁽²⁾VTT Technical Research Center of Finland Ltd., Micronova, Tietotie 3, 02150 Espoo, Finland

Abstract Electro-optic modulator that utilizes the electric-field-induced Pockels effect on a micron-thick silicon photonic platform is demonstrated for the first time. The optimal design delivers a loss-modulation-voltage product of < 5 V·dB. A proof-of-concept device is fabricated to demonstrate 15-Gbps non-return-to-zero modulation using 1.8- μ m-thick all-silicon waveguide. ©2023 The Author(s)

Introduction

Silicon photonics (SiPh) has become the key technology that provides cost-effective photonic integrated circuits for a wide range of applications, including optical communication, switching, computing, and sensing. The prevailing SiPh devices utilize a silicon-on-insulator (SOI) substrate with typically 220-nm-thick silicon layer. However, there is a rising interest in adopting thicker SOI platforms with a micron-scale-thick silicon waveguide^{[1]–[6]}. Compared with the conventional thin SiPh platform, it offers numerous advantages, including ultralow propagation loss (< 0.1 dB/cm), efficient and alignment-tolerant coupling to a cleaved single-mode fiber (SMF), polarization independence, and high saturated optical power. As a result, thick SiPh devices have been widely utilized for datacenter transceivers^[4], polarization-insensitive switches^[5], low-cost wearable sensors^[6], and quantum devices^[3].

Despite many advantages, one of the remaining challenges for the micron-thick SiPh devices is to achieve all-silicon high-speed electro-optic (EO) modulators without integrating III-V or other active materials^[3]. While conventional SiPh high-

speed Mach-Zehnder modulators (MZMs) utilize the carrier depletion effect, such approach cannot be directly implemented due to the difficulty in uniformly doping the thick silicon waveguide. Moreover, traditional carrier-depletion-based modulators inherently suffer from large insertion loss, which spoils the advantage of using the thick SiPh platforms.

Although silicon does not possess a second-order optical nonlinear susceptibility, $\chi^{(2)}$, recent studies have revealed that the electric-field-induced Pockels effect (EPIPE) arises from the third-order nonlinear susceptibility tensor, $\chi^{(3)}$, when a substantial DC electric field is applied^{[7],[8]}. This effect has been used on the 220-nm-thick SiPh platforms to demonstrate second-harmonic generation (SHG)^[7] and high-speed EO modulation^[8] at the cryogenic temperature for quantum applications.

In this work, we utilize this EPIPE to realize high-speed EO phase modulator on a micron-thick SiPh platform for the first time. From comprehensive simulation, our optimal design demonstrates efficient EO modulation with a loss-modulation-voltage product ($V_{\pi}L_{\alpha}$) of 2.3 V·dB under a DC bias of 40 V/ μ m. Then, a proof-

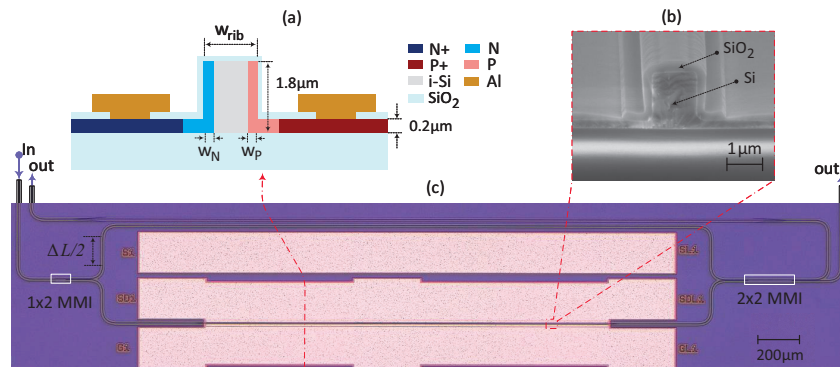


Fig. 1: EPIPE-based phase modulator on 1.8- μ m-thick SiPh platform: (a) Schematic cross-sectional structure, (b) cross-sectional SEM image of the fabricated modulator, and (c) top micro-photograph of the entire asymmetrical MZM circuit. The upper electrode is a dummy pad added for a testing purpose and not used in this experiment.

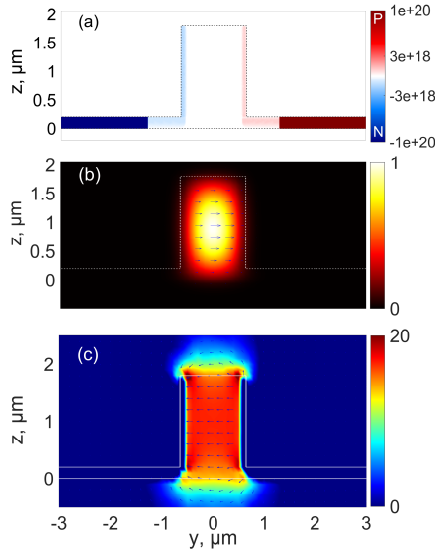


Fig. 2: Optimal design of the EFIPE-based modulator with $w_{\text{rib}} = 1.3 \mu\text{m}$ and $w_{\text{P}} = w_{\text{N}} = 0.2 \mu\text{m}$: (a) Doping profile, (b) optical electric-field profile of the TE mode, and (c) DC electric-field distribution ($\text{V}/\mu\text{m}$) under a reverse bias of 24 V.

of-concept asymmetric MZM is fabricated to experimentally demonstrate 15-Gbps non-return-to-zero (NRZ) signal modulation using a $1.8\text{-}\mu\text{m}$ -thick all-silicon waveguide for the first time to the best of our knowledge.

Modulator Design and Numerical Results

The cross-section of the EFIPE-based phase modulator considered in this work is shown in Fig. 1(a). We assume a silicon rib waveguide with a height of $1.8 \mu\text{m}$ and a pedestal slab thickness of $0.2 \mu\text{m}$ on a $3\text{-}\mu\text{m}$ buried oxide (BOX) layer. The sidewalls of the rib structure are p/n-doped to form a p-i-n junction laterally along the waveguide. By applying a high DC reverse bias to the p-i-n junction, Pockels effect is induced inside the non-doped silicon region^{[7],[8]}, which can be used for high-speed and low-loss phase modulation.

The waveguide dimension and the doping profile are critical in achieving high modulation efficiency with minimal optical loss; the p/n-doped regions at the sidewalls, specified by w_{P} and w_{N} in Fig. 1(a), need to be as narrow as possible to suppress the optical propagation loss, while they need to be thick enough to prevent complete depletion under a high reverse bias. We therefore performed comprehensive numerical optimization by calculating both the carrier distribution and the optical mode profile using Lumerical Charge and EME solvers. The EFIPE was included in the model using the third-order nonlinear susceptibility of silicon ($\chi^{(3)} = 2.8 \times 10^{-19} \text{ m}^2 \text{ V}^{-2}$), given in the literature^[8]. As a realistic doping profile, we assumed p/n doping levels of $< 3 \times 10^{18} \text{ cm}^{-2}$ and

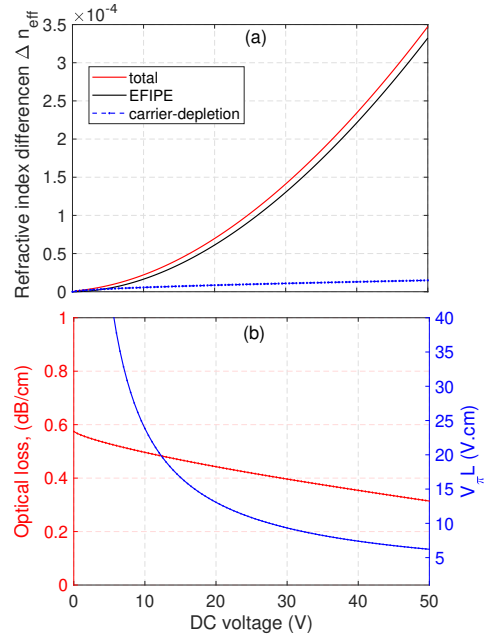


Fig. 3: Simulated phase modulator performance: (a) Effective index change (red) with the contributions from EFIPE (black) and carrier-depletion effect (blue). (b) Optical loss (red) and modulation efficiency (blue) as a function of reverse DC voltage.

p+/n+ doping levels at $1 \times 10^{20} \text{ cm}^{-2}$.

Figure 2 shows the waveguide structure and the doping profile of the obtained design with the waveguide width of $w_{\text{rib}} = 1.3 \mu\text{m}$ and $w_{\text{P}} = w_{\text{N}} = 0.2 \mu\text{m}$. From Fig. 2(b), we can see that the fundamental TE mode is strongly confined inside the rib waveguide, having a small overlap with the p/n regions shown in Fig. 2(a). At the same time, high DC electric field of $\approx 20 \text{ V}/\mu\text{m}$ can be applied across the entire optical mode under 24-V reverse bias as shown in Fig. 2(c).

Figure 3(a) shows the simulated change in the effective refractive index, Δn_{eff} , as a function of applied reverse voltage. We can see that the EFIPE has a dominant contribution compared to the carrier-depletion effect used in the conventional SiPh modulators. Fig. 3(b) shows the optical propagation loss, α , and the modulation efficiency, $V_{\pi}L$. With increasing bias, optical loss decreases as a result of carrier depletion at p/n-doped regions. Under a nominal reverse voltage of 24 V, we obtain $\alpha = 0.42 \text{ dB/cm}$ and $V_{\pi}L = 11.21 \text{ V}\cdot\text{cm}$. This gives a loss-modulation-voltage product of $V_{\pi}L\alpha = 4.7 \text{ V}\cdot\text{dB}$, which is lower than the conventional SiPh carrier-depletion-based phase modulators. Moreover, under 44-V reverse bias, corresponding to the approximate breakdown electric field ($\approx 40 \text{ V}/\mu\text{m}$) of silicon, we obtain $\alpha = 0.34 \text{ dB/cm}$ and $V_{\pi}L = 6.69 \text{ V}\cdot\text{cm}$, and $V_{\pi}L\alpha = 2.3 \text{ V}\cdot\text{dB}$.

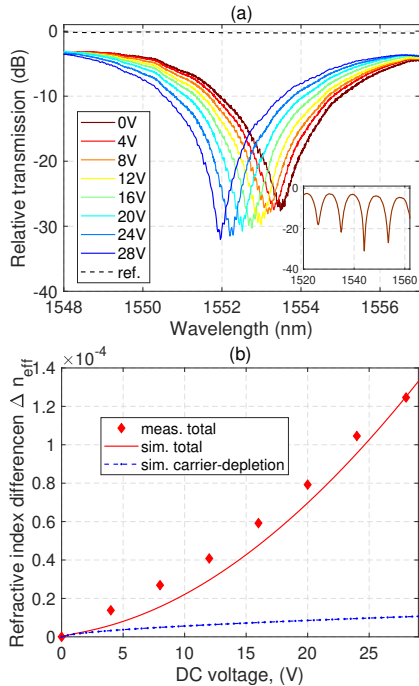


Fig. 4: (a) Optical transmission spectra of asymmetrix MZM measured at different reverse bias voltages. Wider-range spectrum at 0 V is shown in the inset. (b) Measured effective refractive index modulation versus the reverse bias voltage. Simulated results are shown by red and blue lines.

Experimental Results

As a proof-of-concept device, we fabricated asymmetrical MZMs with the EPIFE-based phase modulators, designed in the previous section. The scanning-electron-microscope (SEM) cross-sectional image at the active modulator section and the top photograph of the entire fabricated device are shown in Figs. 1(b) and (c). In this device, the length of the EPIFE-based phase modulator is 2 mm and the unbalanced arm difference of MZM is 200 μm . The n+/p+ regions are separated from the waveguide by 0.8 μm . Travelling-wave Al electrodes are employed to enable high-speed modulation. Note that a dummy Al electrode is added for testing purposes.

Figure 4(a) shows the optical transmission spectra of TE-mode light through the asymmetric MZM measured under an increasing reverse bias. For reference, optical transmission through a straight passive waveguide is also plotted (black dots). The total excess loss of the asymmetric MZM is ≈ 3.5 dB, which accounts for the losses at the 1×2 and 2×2 multimode-interference (MMI) couplers, four Euler bends, and six rib-to-strip waveguide transitions, which were not fully optimized in the current device. From the wavelength shifts observed in Fig. 4(a) and the measured free-spectral range (FSR) of 9.5 nm as shown in the inset, the change in the effective refractive in-

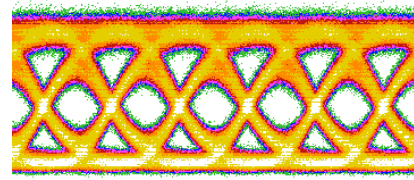


Fig. 5: Observed eye diagram of 15-Gbps NRZ signal modulated at $V_{\text{DC}} = 24$ V and $V_{\text{PP}} = 9.5$ V with 2-mm-long device.

dex is derived and plotted as a function of the reverse voltage in Fig. 4(b). The measured results agree well with the simulation (red solid) and are significantly larger than those induced by the carrier depletion (blue broken).

Finally, Fig. 5 shows the measured eye diagram of the modulated light when the asymmetrix MZM is driven by a 15-Gbps non-return-to-zero (NRZ) signal. The wavelength is 1549.5 nm, while the DC reverse bias and V_{pp} are set to 24 V and 9.5 V, respectively. Open eyes are obtained with an extinction ratio (ER) of 5.9 dB. To the best of our knowledge, this is the highest-speed modulation achieved by an all-silicon modulator fabricated on a micron-scale-thick SiPh platform. On the other hand, the current device suffered from a low breakdown voltage of around 29 V. This needs to be increased through further optimization of the device design and fabrication process to achieve the improved performance as predicted from Fig. 3. In addition, by optimizing the travelling-wave electrode design, higher-speed operation is expected.

Conclusions

We have numerically and experimentally demonstrated EPIFE-based phase modulator on a micron-thick SiPh platform for the first time. Owing to the strong modal confinement inside the thick silicon waveguide with a small overlap with the p/n-doped region, low-loss modulation can be obtained with a simulated $V_{\pi}L\alpha = 2.3$ V·dB at the breakdown electric field of 40 V/ μm . Using a fabricated MZM with 1.8- μm -thick waveguide, we successfully demonstrated 15-Gbps NRZ signal modulation with a clear evidence of EPIFE. This work demonstrates the promise of thick SiPh platforms for high-speed and energy-efficient communication, quantum computing, and sensing applications.

Acknowledgements

This work was obtained from the commissioned research 21801 by the National Institute of Information and Communications Technology (NICT), Japan.

References

- [1] T. Aalto, M. Cherchi, M. Harjanne, *et al.*, “Open-access 3- μm SOI Waveguide Platform for Dense Photonic Integrated Circuits”, *IEEE Journal of Selected Topics in Quantum Electronics*, vol. 25, no. 5, pp. 1–9, 2019. DOI: 10.1109/JSTQE.2019.2908551.
- [2] A. J. Zilkie, P. Srinivasan, A. Trita, *et al.*, “Multi-micron silicon photonics platform for highly manufacturable and versatile photonic integrated circuits”, *IEEE Journal of Selected Topics in Quantum Electronics*, vol. 25, no. 5, pp. 1–13, 2019. DOI: 10.1109/JSTQE.2019.2911432.
- [3] M. Cherchi, A. Bera, A. Kemppinen, *et al.*, “Supporting quantum technologies with an ultralow-loss silicon photonics platform”, *Advanced Photonics Nexus*, vol. 2, no. 2, p. 024002, 2023. DOI: 10.1117/1.APN.2.2.024002.
- [4] A. H. Talkhooncheh, A. Zilkie, G. Yu, R. Shafiiha, and A. Emami, “A 200Gb/s QAM-16 silicon photonic transmitter with 4 binary-driven EAMs in an MZI structure”, in *Optical Fiber Communication Conference (OFC) 2023*, Optica Publishing Group, 2023, M1E.6. [Online]. Available: <https://opg.optica.org/abstract.cfm?URI=OFC-2023-M1E.6>.
- [5] Y. Wang, S. Bhat, B. Shi, T. Aalto, and N. Calabretta, “C- and L-band low polarization sensitive nanosecond 1×2 electro-optic MZI switch on 3- μm thick silicon platform”, in *Optical Fiber Communication Conference (OFC) 2023*, Optica, 2023, M4J.3. [Online]. Available: <https://opg.optica.org/abstract.cfm?URI=OFC-2023-M4J.3>.
- [6] J. B. Driscoll, P. Perea, A. Kauffman, A. J. Zilkie, and B. V. Steeg, “Pioneering silicon photonics for wearable sensors”, in *Optical Fiber Communication Conference (OFC) 2023*, Optica Publishing Group, 2023, Th1A.6. [Online]. Available: <https://opg.optica.org/abstract.cfm?URI=OFC-2023-Th1A.6>.
- [7] E. Timurdogan, C. V. Poulton, M. J. Byrd, and M. R. Watts, “Electric field-induced second-order nonlinear optical effects in silicon waveguides”, *Nature Photonics*, vol. 11, no. 3, pp. 200–206, Mar. 2017, ISSN: 1749-4893. DOI: 10.1038/nphoton.2017.14.
- [8] U. Chakraborty, J. Carolan, G. Clark, *et al.*, “Cryogenic operation of silicon photonic modulators based on the dc kerr effect”, *Optica*, vol. 7, no. 10, pp. 1385–1390, Oct. 2020. DOI: 10.1364/OPTICA.403178.